Inorg. Chem. **2008**, *47*, 4579−4590

Bis(α-diimine)iron Complexes: Electronic Structure Determination by Spectroscopy and Broken Symmetry Density Functional Theoretical Calculations

Nicoleta Muresan,[†] Connie C. Lu,[†] Meenakshi Ghosh,[†] Jonas C. Peters,[‡] Megumi Abe,[‡] Lawrence M. Henling,[‡] Thomas Weyhermöller,[†] Eckhard Bill,[†] and Karl Wieghardt*[,†]

Max-Planck Institute for Bioinorganic Chemistry, Stiftstrasse 34−36, D-45470 Mülheim an der Ruhr, Germany, and Division of Chemistry and Chemical Engineering, Arnold and Mabel Beckman Laboratories of Chemical Synthesis, California Institute of Technology, Pasadena, California 91125

Received November 19, 2007

The electronic structure of a family comprising tetrahedral (α-diimine)iron dichloride, and tetrahedral bis(α-diimine)iron compounds has been investigated by Mössbauer spectroscopy, magnetic susceptibility measurements, and X-ray crystallography. In addition, broken-symmetry density functional theoretical (B3LYP) calculations have been performed. A detailed understanding of the electronic structure of these complexes has been obtained. A paramagnetic ($S_t = 2$), tetrahedral complex $[Fe^{II}(^4L)_2]$, where $(^4L)^{1-}$ represents the diamagnetic monoanion *N-tert*-butylquinolinylamide, has been synthesized and characterized to serve as a benchmark for a Werner-type complex containing a tetrahedral $Fe^{II}N_4$ geometry and a single high-spin ferrous ion. In contrast to the most commonly used description of the electronic structure of bis(α-diimine)iron(0) complexes as low-valent iron(0) species with two neutral α-diimine ligands, it is established here that they are, in fact, complexes containing two $(\alpha\text{-diiminato})^{1-\bullet}$ π radical monoanions and a high-spin ferrous ion (in tetrahedral N_4 geometry) ($S_{Fe} = 2$). Intramolecular antiferromagnetic coupling between the π radical ligands ($S_{rad} = {}^1/_2$) and the ferrous ion ($S_{Fe} = 2$) yields the observed $S_t = 1$ ground state. The study confirms that α-diimines are redox noninnocent ligands with an energetically low-lying antibonding π^* lowest unoccupied molecular orbital which can accept one or two electrons from a transition metal ion. The (α-diimine)$FeCl_2$ complexes ($S_t = 2$) are shown to contain a neutral α-diimine ligand, a high spin ferrous ion, and two chloride ligands.

Introduction

In 1977 tom Dieck and Bruder[1] reported the synthesis of an interesting series of bis(α-diimine)iron complexes which they prepared by the reaction of $FeCl_2$ with 2 equiv of an α-diimine ligand under reducing conditions (2 equiv of sodium) in diethylether. The electronic structure of these violet, monomeric, putatively tetrahedral, and paramagnetic ($S = 1$) complexes $[FeL_2]$ has ever since[1−4] been described as zerovalent iron species (d^8, $S = 1$ in a tetrahedral ligand field) containing two neutral α-diimine ligands.

We note that tom Dieck et al.[2] indicated the possibility of a more complex electronic structure involving a divalent, high-spin ferrous ion ($S_{Fe} = 2$) N,N′-coordinated to two π radical monoanions ($S_{rad} = {}^1/_2$) which are intramolecularly spin coupled yielding the observed triplet ground state, but they did not provide any spectroscopic or crystallographic evidence.

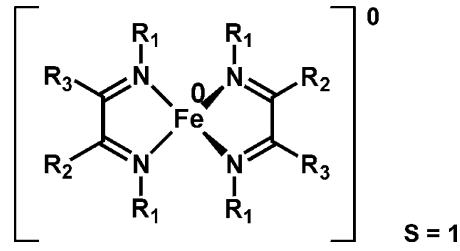

In 2005 Chirik et al.[4a] reported the first crystal structure of such bis(α-diimine)iron species. The quality of this

* To whom correspondence should be addressed. E-mail: wieghardt@mpi-muelheim.mpg.de.
† Max-Planck-Institute for Bioinorganic Chemistry.
‡ California Institute of Technology.

(1) tom Dieck, H.; Bruder, H. *J. Chem. Soc., Chem. Commun.* **1977**, 24.
(2) tom Dieck, H.; Diercks, R.; Stamp, L.; Bruder, H.; Schuld, T. *Chem. Ber.* **1987**, *120*, 1943.

10.1021/ic7022693 CCC: $40.75
Published on Web 04/29/2008

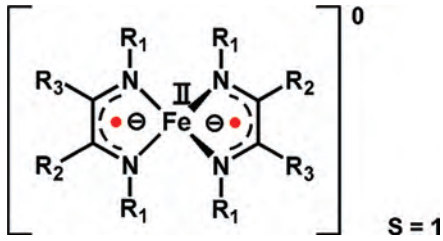

structure determination does not allow a detailed discussion of C−N, C−C, and Fe−N distances. Nevertheless, these authors concluded from an analysis of the structural data of this and similar species[4a,b] that a description of the electronic structure as intermediate spin *ferrous* species ($S_{Fe} = 1$) with "an important contribution" from the diamagnetic "ene-diamide" and the neutral diamagnetic α-diimine canonical form is appropriate.

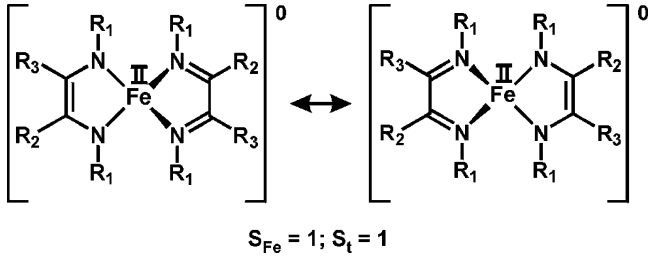

It is worth mentioning that a fourth electronic structure should also be considered which involves an intermediate spin ferric ion ($S_{Fe} = 3/2$), a monoanionic π-radical, and a diamagnetic dianion.

Bis(α-diimine)iron complexes are important species because they are known to initiate catalytic atom-transfer radical polymerization,[5] the dimerization of dienes,[6] and the polymerization of olefins.[7]

We decided to synthesize a new series of such complexes using the α-diimine ligands shown in Scheme 1, namely $(^1L^{Ox})^0$, $(^2L^{Ox})^0$, and $(^3L^{Ox})^0$.

The ligand abbreviations were chosen to highlight the fact that neutral α-diimines may be reduced in two single one-electron steps generating the paramagnetic π radical monoanions $(^xL^{\bullet})^{1-}$ (x = 1,2,3) and the diamagnetic dianions $(^xL^{Red})^{2-}$; a single resonance structure of each form is shown in Scheme 2.

Scheme 1

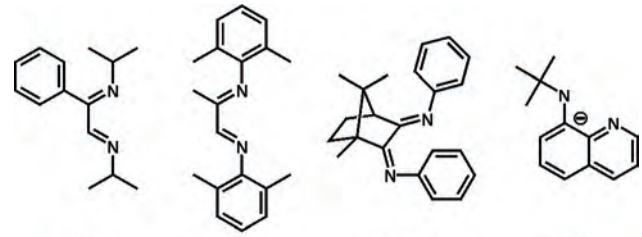

$[Fe^{II}(^4L)_2]$	S = 2	(1)
$[Fe^{II}(^1L^{OX})Cl_2]$	S = 2	(2)
$[Fe^{II}(^1L^{\bullet})_2]$	S = 1	(3)
$[Fe^{II}(^2L^{OX})Cl_2]$	S = 2	(4)
$[Fe^{II}(^2L^{\bullet})_2]$	S = 1	(5)
$[Fe^{II}(^3L^{\bullet})_2]$	S = 1	(6)

Scheme 2

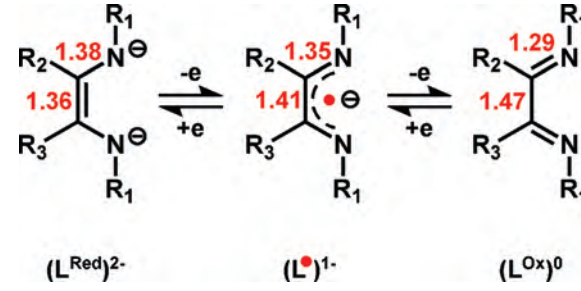

It is well established from careful X-ray crystallographic studies of Zn-complexes that the ligand oxidation level differs clearly in their respective C−N bond lengths (and also the C−C bond distances).[8–10]

Recently, it has been shown that the neutral complexes of some tetrahedral bis(α-diimine)nickel complexes possess an electronic structure which is best described as nickel(II) (d^8, $S_{Ni} = 1$ in tetrahedral ligand field) with two N,N′-coordinated monoanionic ligand π radicals $(L^{\bullet})^{1-}$ yielding a diamagnetic ground state.[11,12]

Finally, we have reinvestigated some of Chirik's complexes, namely those shown in Scheme 3 (**7**, **8**, and **9**). We have recorded their zero-field Mössbauer spectra and conclude that

(3) Walther, D.; Kreisel, G.; Kirmse, R. *Z. Anorg. Allg. Chem.* **1982**, *487*, 149.
(4) (a) Bart, S. C.; Hawrelak, E. J.; Lobkovsky, E.; Chirik, P. J. *Organometallics* **2005**, *24*, 5518. (b) Bart, S. C.; Hawrelak, E. J.; Schmisseur, A. K.; Lobkovsky, E.; Chirik, P. J. *Organometallics* **2004**, *23*, 237.
(5) (a) Gibson, V. C.; O'Reilly, R. K.; Wass, D. F.; White, A. J. P.; Williams, D. J. *Macromolecules* **2003**, *36*, 2591. (b) Gibson, V. C.; O'Reilly, R. K.; Reed, W.; Wass, D. F.; White, A. J. P.; Williams, P. J. *Chem. Commun.* **2002**, 1850.
(6) (a) tom Dieck, H.; Stamp, L.; Diercks, R.; Müller, C. *New J. Chem.* **1985**, *9*, 289. (b) Le Floch, P.; Knoch, F.; Kremer, F.; Mathey, F.; Scholz, J.; Scholz, W.; Thiele, K.-H.; Zenneck, U. *Eur. J. Inorg. Chem.m* **1998**, 119.
(7) Lorber, C; Choukroun, R.; Costes, J.-P.; Donnadien, B. C. *C. R. Chim.* **2002**, *5*, 251.
(8) van Koten, G.; Vrieze, K. *Adv. Organomet. Chem.* **1982**, *21*, 151.
(9) Gardiner, M. G.; Hanson, G. R.; Henderson, M. J.; Lee, F. C.; Raston, C. L. *Inorg. Chem.* **1994**, *33*, 2456.
(10) Rijnberg, E.; Richter, B.; Thiele, K.-H.; Boersma, J.; Veldman, N.; Spek, A. L.; van Koten, G. *Inorg. Chem.* **1998**, *37*, 56.
(11) Khusniyarov, M. M.; Harms, K.; Burghaus, O.; Sundermeyer, J. *Eur. J. Inorg. Chem.* **2006**, *15*, 2985.

Scheme 3

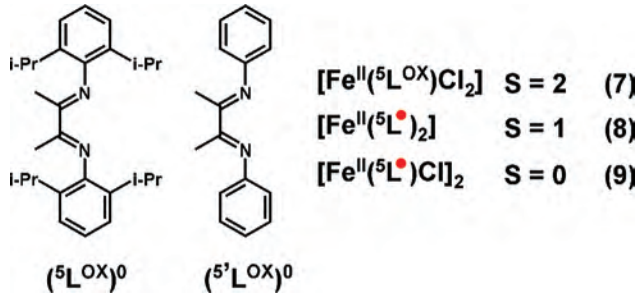

none of these contain a low-valent iron ion with a formal oxidation number of 0 or +1. Instead, all of them are identified as high-spin ferrous complexes (d^6, $S_{Fe} = 2$) with zero (**7**), one (**9**), and two (**8**) ligand π radical monoanionic α-diimine ligands per metal. Note that **9** is a dimer with two μ-chloro bridges, and intramolecular antiferromagnetic exchange coupling is anticipated. Therefore, we have investigated the temperature dependence of its magnetic properties.

Experimental Section

All air-sensitive materials were manipulated under a N_2 or Ar blanketing atmosphere by using standard Schlenk line procedures or a glovebox. All commercially available chemicals were used as received. The ligands 2-phenyl-1,4-bis(isopropyl)-1,4-diazabutadiene ($^1L^{Ox})^0$, 2-methyl-1,4-bis(2,6-diisopropylphenyl)-1,4-diaza-1,3-butadiene ($^2L^{Ox}$), and enantiopure *R*-(-)-bis(phenylimino)camphene ($^3L^{Ox})^0$ were synthesized according to published procedures.[13a–c] Chirik's complexes **7**, **8**, and **9** have been synthesized as described in refs 4a and 4b.

Synthesis of *N-tert*-Butylquinolinylamine, H(^{4}L). $Pd(OAc)_2$ (151.1 mg, 0.629 mmol) and BINAP (419 mg, 0.629 mmol) were preheated at 85 °C for 30 min in 15 mL of toluene. The mixture was added to a 250 mL reaction bomb flask containing bromoquinoline (7.0 g, 33.64 mmol), *tert*-butylamine (3.691 g, 50.47 mmol), and sodium *tert*-butoxide (4.527 g, 47.1 mmol) in 75 mL of toluene. The resulting reaction mixture was dark purple. The reaction bomb was sealed with a Teflon cap and heated at 110 °C for 48 h. The solution was then cooled to room temperature in air, diluted with 200 mL of dichloromethane, and washed with H_2O (3 × 200 mL) and brine (2 × 150 mL). The organic layer was collected, dried over $MgSO_4$, and filtered over celite. Removal of solvent in vacuo yielded a dark brown oil, which was purified by flashing through a column of silica with dichloromethane as the eluant. Dichloromethane is removed in vacuo to yield a bright orange-yellow oil (6.318 g, 94%). ^{1}H NMR ($CDCl_3$, 300 MHz): δ 8.69 (dd, $J_1 = 4.0$ Hz, $J_2 = 1.6$ Hz, 1H); 8.03 (dd, $J_1 = 8.0$ Hz, $J_2 = 1.6$ Hz, 1H); 7.37-7.32 (m, 2H); 7.00 (t, $J_1 = 8.0$ Hz, $J_2 = 4.0$ Hz, 1H); 6.94 (dd, $J_1 = 8.0$ Hz, $J_2 = 4.0$ Hz, 1H); 6.45 (s, 1H, N*H*); 1.54 (s, 9H, *t*-butyl); GC-MS: $m/z = 200$.

Preparation of Lithium *N-tert*-Butylquinolinylamide, Li(^{4}L). 1.6 M *n*BuLi (5.93 mL, 9.49 mmol) was added dropwise to a stirring solution of *tert*-butylquinolinylamine (2.00 g, 9.99 mmol) in 75 mL of petroleum ether at −78 °C under nitrogen. Upon addition of *n*BuLi, red-orange lithium *tert*-butylquinolinylamide precipitated from the reaction. The reaction was warmed up to 0 °C, and the solvent removed in vacuo to yield a red solid. In the dry box, the red solid was washed with petroleum ether (3 × 20 mL) to yield a bright orange powder (1.83 g, 94%). Protonation with H_2O and analysis by GC-MS showed only *N-tert*-butyl-quinolinylamine.

Synthesis of Complexes. $[Fe^{II}(^4L)_2]$ (1). Lithium *N-tert*-butylquinolinylamide (1.2 g, 5.82 mmol) dissolved in 20 mL of tetrahydrofuran was added to a stirring suspension of $FeCl_2$ (368.8 mg, 2.91 mmol) in 30 mL of tetrahydrofuran. After stirring at room temperature overnight, a dark red-brown homogeneous solution was obtained. Tetrahydrofuran was removed in vacuo to yield dark red solids. The dark red solids were washed with petroleum ether and stirred in 25 mL of toluene overnight. The toluene solution was filtered over a frit, and dark red solids were collected. Solids were washed with toluene (4 × 20 mL) until only a gray powder remained. Toluene was removed in vacuo to yield a dark red-brown powder. The powder was then washed with 10% benzene in petroleum ether (4 × 5 mL), 20% benzene in petroleum ether (4 × 5 mL), and 30% benzene in petroleum ether (1 × 5 mL), and dried in vacuo (0.819 g, 62%). ^{1}H NMR (C_6D_6, 300 MHz): δ 64.02 (s); 61.21 (bs); 52.88 (s); −7.42 (s); −51.31 (s); −55.35 (s). Evans Method (C_6D_6, 298 K): 4.8 μ_B Anal. Calcd for $C_{26}H_{30}N_4Fe$: C, 68.7; H, 6.6; N, 12.3. Found: C, 68.9; H, 6.6; N, 12.5.

$Fe^{II}(^1L^{Ox})Cl_2$] (2). To a solution of 2-phenyl-1,4-bis(isopropyl)-1,4-diazabutadiene (0.5 g, 2.31 mmol) in tetrahydrofuran (20 mL) under an argon blanketing atmosphere was added 0.29 g of $FeCl_2$ (2.31 mmol). The deep violet solution was stirred for 20 h at room temperature. The solvent was removed by evaporation under reduced pressure, and the residue was washed with toluene. Complex **2** was isolated as a dark violet solid (0.75 g, 2.18 mmol, 94%). X-ray quality crystals were obtained by slow evaporation of the solvent from a concentrated solution of **2** in tetrahydrofuran. Anal. Calcd for $C_{14}H_{20}N_2FeCl_2$: C, 49.1; H, 5.8; N, 8.2; Fe, 16.3; Cl, 20.7. Found: C, 49.1; H, 6.0; N, 7.9; Fe, 16.1; Cl, 20.5.

$[Fe^{II}(^1L)_2]$ (3). To a solution of **2** (0.6 mg, 1.75 mmol) in *n*-hexane (30 mL) was added sodium (80 mg, 3.50 mmol) with stirring at 20 °C. After 10 min., a solution of 2-phenyl-1,4-bis(isopropyl)-1,4-diazabutadiene (0.37 g, 1.75 mmol) in *n*-hexane (10 mL) was added, and the reaction mixture was stirred for 24 h. The dark violet color of the solution turned to dark brown. The solvent was removed by evaporation under reduced pressure to give a dark brown precipitate which was washed with acetonitrile and dried in vacuo. Yield: 0.76 g (89%). Anal. Calcd for $C_{28}H_{40}N_4Fe$: C, 68.8; H, 8.2; N, 11.5; Fe, 11.4. Found: C, 68.8; H, 8.5; N, 11.3; Fe, 11.1.

$[Fe^{II}(^2L^{Ox})Cl_2]$ (4). To a solution of 2-methyl-1,4-bis(2,6-diisopropylphenyl)-1,4-diaza-1,3-butadiene (0.5 g, 1.79 mmol) in tetrahydrofuran (20 mL) under an argon blanketing atmosphere was added 0.22 g of $FeCl_2$ (1.79 mmol). The deep blue solution was stirred for 20 h at room temperature. The solvent was removed by evaporation under reduced pressure, and the residue was washed with toluene to remove any soluble impurities. Complex **4** was isolated as a brown solid (0.70 g, 1.72 mmol, 97%). Anal. Calcd

(12) (a) Muresan, N.; Chlopek, K.; Weyhermüller, T.; Neese, F.; Wieghardt, K. *Inorg. Chem.* **2007**, *46*, 5327. (b) Blanchard, S.; Neese, F.; Bothe, E.; Bill, E.; Weyhermüller, T.; Wieghardt, K. *Inorg. Chem.* **2005**, *44*, 3636. (c) Chlopek, K.; Bothe, E.; Neese, F.; Weyhermüller, T.; Wieghardt, K. *Inorg. Chem.* **2006**, *45*, 6298.

(13) (a) Armesto, D.; Bosch, P.; Gallego, M. G.; Martin, J. F.; Ortiz, M. J.; Perez-Ossorio, R.; Ramos, A. *Org. Prep. Proced. Int.* **1987**, *19*, 181. (b) Druzhkov, N. O.; Teplova, I. A.; Glushakova, V. N.; Skorodumova, N. A.; Abakumov, G. A.; Zhao, B.; Berluche, E.; Schulz, D. N.; Baugh, L. S.; Ballinger, C. A.; Squire, K. R.; Canich, J.-A. M.; Bubnov, M. P. O. S. Patent: PCT/U.S. Patent 022356, 2003; WO Patent 007509, 2004. (c) van Asselt, R.; Elsevier, C. J.; Smeets, W. J. J.; Spek, A. L.; Benedix, R *Rec. Trav. Chim. (Pays Bas)* **1994**, *113*, 88.

for $C_{19}H_{22}N_2FeCl_2$: C, 56.3; H, 5.4; N, 6.9; Fe, 13.8. Found: C, 56.1; H, 5.3; N, 7.0; Fe, 13.8.

$[Fe^{II}(^2L)_2]$ (5). To a solution of **4** (0.6 mg, 1.48 mmol) in *n*-hexane (30 mL) was added sodium (68 mg, 2.96 mmol) with stirring at 20 °C. After 10 min, a solution of 2-methyl-1,4-bis(2,6-diisopropylphenyl)-1,4-diaza-1,3-butadiene (0.41 g, 1.48 mmol) in *n*-hexane (10 mL) was added, and the reaction mixture was stirred for 24 h. The dark blue color of the solution turned to dark green. The solvent was removed by evaporation under reduced pressure to give a dark green precipitate which was washed with acetonitrile and dried in vacuo. Yield: 0.76 g (80%). Anal. Calcd for $C_{38}H_{44}N_4Fe$: C, 74.53; H, 7.24; N, 9.15; Fe, 9.12. Found: C, 74.0; H, 7.30; N, 9.15; Fe, 9.20.

$[Fe^{II}(^3L^{\bullet})_2]$ (6). Two equiv of the ligand (1R)-(-)-(phenylimino)camphane (778 mg, 2.45 mmol), 1 equiv of $FeCl_2$ (159 mg, 1.23 mmol), and 2.05 equiv of sodium metal (58.0 mg, 2.52 mmol) were added to a glass vessel. Dimethoxyether (DME, 10 mL) was added, and the reaction mixture was vigorously stirred for 18 h. The solvent was then completely removed under reduced pressure. Pentane (2 mL) was added to the crude residue, which was then dried further under reduced pressure. The dried residue was washed with pentane (2 × 3 mL), extracted with C_6H_6, filtered through celite, and subjected to reduced pressure for solvent removal. A dark-brown powder was thus obtained. Single crystals of X-ray quality were grown from vapor diffusion of pentane into a concentrated C_6H_6 solution of **6**. Yield: 711 mg (84%). Anal. Calcd for $C_{44}H_{48}FeN_4$: C, 76.73; H, 7.02; N, 8.13. Found: C, 76.6; H, 7.1; N, 8.2.

X-ray Crystallography. X-Ray Crystallographic Data Collection and Refinement of the Structures. A dark red single crystal of **1**, a pink colored crystal of **2**, and a brown specimen of **6** were coated with perfluoropolyether, picked up with nylon loops and mounted in the nitrogen cold stream of the diffractometers. A Bruker-Nonius KappaCCD diffractometer equipped with a Mo-target rotating-anode X-ray source was used in case of **2** and **6**, and a Bruker Smart 1000 CCD diffractometer with a sealed tube source was used for compound **1**. Graphite monochromated Mo Kα radiation (λ =0.71073 Å) was used throughout. Final cell constants were obtained from least-squares fits of all measured reflections. Intensity data were corrected for absorption using intensities of redundant reflections. The structures were readily solved by Patterson methods and subsequent difference Fourier techniques. The Siemens ShelXTL[14] software package was used for solution and artwork of the structures; ShelXL97[15] was used for the refinement. All non-hydrogen atoms were anisotropically refined, and hydrogen atoms were placed at calculated positions and refined as riding atoms with isotropic displacement parameters. Crystallographic data of the compounds are listed in Table 1.

Compound **6** crystallizes in the chiral space-group $P2_1$, and the unit cell was found to contain two crystallographically independent molecules. Refinement of the structure revealed that cocrystallization of the two possible enantiomerically pure geometrical isomers (cisoid and transoid) occurred for both positions, but only one of the two ligands in each independent molecule is statically disordered. The occupation factors refined to a ratio of about 50% for the trans- and the cis-isomer. The absolute structure parameter refined to a value of 0.036 (0.008), and the obtained structure matches nicely the absolute configuration of the employed ligand. It was assumed that the metrical parameters of the ligand are not significantly influenced by the coordination mode (cis or trans), and therefore, the ligand substructures within each disordered position were restrained to be equal within errors using the SAME instruction of ShelXL97. In addition, equal anisotropic displacement parameters were used for corresponding atoms giving a total of 139 restraints.

Table 1. Crystallographic Data for **1**, **2**, and **6**

	1	**2**	**6**
chem. formula	$C_{26}H_{30}FeN_4$	$C_{14}H_{20}Cl_2FeN_2$	$C_{44}H_{48}FeN_4$
fw	454.39	343.07	688.71
space group	*C*2/*c*, No. 15	$P\bar{1}$, No. 2	$P2_1$, No. 4
a, Å	17.8934(14)	7.4721(3)	14.1374(3)
b, Å	14.2722(11)	9.9945(5)	13.7276(3)
c, Å	17.8740(14)	11.9345(5)	19.2999(5)
α, deg	90	71.501(3)	90
β, deg	91.372(1)	78.244(3)	96.481(3)
γ, deg	90	87.333(3)	90
V, Å	4563.3(6)	827.33(6)	3721.6(2)
Z	8	2	4
T, K	98(2)	100(2)	120(2)
ρ calcd, g cm^{-3}	1.323	1.377	1.229
refl.collected/2Θ$_{max}$	33432/56.90	22997/70.00	110059/67.00
unique refl./$I > 2\sigma(I)$	5356/4372	7265/6505	29054/26787
no. of params/restr.	287/0	176/0	1029/139
λ, Å/μ(Kα), cm^{-1}	0.71073/6.81	0.71073/12.23	0.71073/4.41
R1[a]/goodness of fit[b]	0.0361/2.259	0.0291/1.023	0.0512/1.045
wR2[c] ($I > 2\sigma(I)$)	0.0689	0.0676	0.1262
residual density, e Å^{-3}	+0.87/−0.48	+0.58/−0.39	+0.43/−0.54

[a] Observation criterion: $I > 2\sigma(I)$. R1 = $\Sigma||F_o|-|F_c||/\Sigma|F_o|$. [b] GOF = $[\Sigma[w(F_o^2 - F_c^2)^2]/(n-p)]^{1/2}$. [c] wR2 = $[\Sigma[w(F_o^2 - F_c^2)^2]/\Sigma[w(F_o^2)^2]]^{1/2}$ where $w = 1/\sigma^2(F_o^2) + (aP)^2 + bP$, $P = (F_o^2 + 2F_c^2)/3$.

Physical Measurements. Magnetic susceptibility data were measured from a powder sample in the temperature range 2−300 K by using a SQUID susceptometer (MPMS-7, Quantum Design) with a field of 1.0 T. The experimental data were corrected for underlying diamagnetism by use of tabulated Pascal's constants, as well as for temperature-independent paramagnetism. The susceptibility data of **9** were simulated with our own program julX for exchange coupled systems (see Supporting Information). The simulations are based on the spin-Hamiltonian operator for a linear tetranuclear system of two high-spin Fe(II) with spin $S_2 = 2$, $S_3 = 2$, and two terminal ligand radicals with $S_1 = {}^1/_2$, $S_4 = {}^1/_2$.

$$\hat{H} = -2J[\hat{S}_1 \cdot \hat{S}_2 + \hat{S}_3 \cdot \hat{S}_4] - 2J' \hat{S}_2 \cdot \hat{S}_3 + g\beta(\hat{S}_2 \cdot \hat{S}_3)\cdot\vec{B} + g\beta(\hat{S}_1 + \hat{S}_4)\cdot\vec{B} + \sum_{i=2,3} D[\hat{S}_{i,z}^2 - (1/3)S(S+1) + (E/D)(\hat{S}_{i,x}^2 - \hat{S}_{i,y}^2)] \quad (1)$$

Here J and J' are the exchange coupling constants for the iron-radical and the iron−iron coupling, respectively; g and g' are the average electronic g values for iron and radicals, and D and E/D are the axial zero-field splitting and rhombicity parameters for iron. The magnetic moments were obtained from the first order derivative of the eigenvalues of eq 1.

The equipment used for the IR, UV−vis, and Mössbauer spectroscopies has been described previously (Ghosh, P.; Bill, E.; Weyhermüller, T.; Wieghardt, K. *J. Am. Chem. Soc.* **2003**, *125*, 3967 and Ray, K.; Bill, E.; Weyhermüller, T.; Wieghardt, K. *J. Am. Chem. Soc.* **2005**, *127*, 5641).

Calculations. All calculations were performed by using the ORCA program package.[16] The geometry optimizations were

(14) *ShelXTL* Version 6.14; Bruker AXS Inc.: Madison, WI, 2003.
(15) Sheldrick, G. M. *ShelXL97*, University of Göttingen: Göttingen, Germany, 1997.
(16) Neese, F. *ORCA, an Ab Initio, Density Functional and Semiempirical Electronic Structure Program Package*, Version 2.4, Revision 36; Max-Planck-Institut für Bioanorganische Chemie: Mülheim/Ruhr, Germany, May 2005.

carried out at the B3LYP level[17] of density-functional theory (DFT). The all-electron Gaussian basis sets were those reported by the Ahlrichs group.[18,19] Triple-ζ quality basis sets with one set of polarization functions on the iron and nitrogen atoms were used (TZVP).[19] The carbon and hydrogen atoms were described by slightly smaller polarized split-valence SV(P) basis sets that are double-ζ quality in the valence region and contain a polarizing set of d-functions on the non-hydrogen atoms.[18] The auxiliary basis sets for all complexes used to expand the electron density in the calculations were chosen to match the orbital basis. The self-consistent field (SCF) calculations were tightly converged (1×10^{-8} Eh in energy, 1×10^{-7} Eh in the density change, and 1×10^{-7} in the maximum element of the DIIS error vector). The geometries were considered converged after the energy change was less than 5×10^{-6} Eh, the gradient norm and maximum gradient element were smaller than 1×10^{-4} Eh/Bohr and 3×10^{-4} Eh/Bohr, respectively, and the root-mean square and maximum displacements of atoms were smaller than 2×10^{-3} Bohr and 4×10^{-3} Bohr, respectively. Corresponding orbitals[20] and density plots were obtained by the program Molekel.[21]

Nonrelativistic single point calculations on the optimized geometries of iron complexes with the B3LYP functional were carried out to predict Mössbauer spectral parameters (isomer shift and quadrupole splitting). These calculations employed the CP(PPP) basis set[22] for iron and the TZV(P) basis sets for N atoms. The SV(P) basis sets were used for the remaining atoms. The Mössbauer isomer shifts were calculated from the computed electron densities at the iron centers as previously described.[23]

Throughout this paper we describe our computational results of iron complexes containing noninnocent ligands using the broken symmetry (BS) approach.[24–26] Recently, the BS approach was successfully applied for transition-metal-containing complexes in the groups of Wieghardt and Neese[27–33] and others.[25,34]

Because for the complexes studied in this work, one can obtain broken-symmetry (BS) solutions to the spin-unrestricted Kohn−Sham equations, we will adopt the following notation: the system is divided into two fragments. The notation BS(*m,n*) refers to a broken symmetry state with *m* unpaired spin-up electrons on fragment 1 and *n* unpaired spin-down electrons essentially localized on fragment 2. In most cases fragments 1 and 2 correspond to the metal and the ligand, respectively. Note that in this notation a standard high-spin open-shell solution would be written down as BS($m+n$,0). In general, The BS(*m,n*) notation refers to the initial guess to the wave function. The variational process does, however, have the freedom to converge to a solution of the form BS($m-n$,0) where effectively the *n*-spin-down electrons pair with $n < m$ spin-up electrons on the partner fragment. Such a solution is then a standard $M_S = (m - n)/2$ unrestricted Kohn−Sham solution. As explained elsewhere,[20] the nature of the solution is investigated via the corresponding orbital transformation, which via the corresponding orbital overlaps displays whether the system is to be described as a spin-coupled or a closed-shell solution.

Results and Discussion

Synthesis of Complexes. Scheme 1 summarizes the ligands and the new complexes **1**−**6**, and Scheme 3 shows the ligands and the revisited complexes **7**−**9** reported by Chirik and co-workers.[4]

The reaction of $FeCl_2$ in dry tetrahydrofuran with 2 equiv of lithium *tert*-butylquinolinylamide (Li(^{4}L), Scheme 1) affords a dark red solid of [Fe^{II}(^{4}L)$_2$] (**1**) upon evaporation of the solvent. The effective magnetic moment of **1** has been determined by NMR spectroscopy (Evans method in C_6D_6) to be 4.5 μ_B at 298 K which indicates the expected high spin $S = 2$ ground-state for **1**. As shown by X-ray crystallography, the high-spin ferrous ion is in a nearly regular tetrahedral environment of 4 nitrogen donor atoms. The two bidentate ligands are the redox-innocent, closed shell, monoanion *tert*-butylquinolinylamide(1−), (^{4}L)$^{1-}$.

Similarly, the reaction of $FeCl_2$ in dry tetrahydrofuran under strictly anaerobic conditions with 1 equiv of an α-diimine, ($^1L^{Ox}$)^0 or ($^2L^{Ox}$) (Scheme 1), yields the neutral, dark-violet, tetrahedral complexes [Fe^{II}($^1L^{Ox}$)Cl_2] (**2**) and [Fe^{II}($^2L^{Ox}$)Cl_2] (**4**), respectively. Temperature dependent (3−300 K) magnetic susceptibility measurements of solid **2** and **4** in an 1.0 T magnetic field shown in Figure 1 for **4** reveal again an $S = 2$ ground state (high spin ferrous ions). Table 2 summarizes the spin Hamiltonian parameters.

Using the same conditions as tom Dieck and Bruder[1] described for the synthesis of their neutral bis(α-diimine)iron complexes, namely, the reaction of 2 equiv of the ligand ($^1L^{Ox}$)^0, ($^2L^{Ox}$)^0, and enantiopure ($^3L^{Ox}$)^0 with 1 equiv of $FeCl_2$and 2 equiv of sodium in *n*-hexane and DME respectively, under an argon atmosphere, the following brown-green complexes were obtained in good yields: [Fe^{II}($^1L^{\bullet}$)$_2$] (**3**), [Fe^{II}($^2L^{\bullet}$)$_2$] (**5**), and [Fe^{II}($^3L^{\bullet}$)$_2$] (**6**). It is also possible to generate **3** and **5** from **2** and **4** by addition of 2 equiv of ($^1L^{Ox}$) and ($^2L^{Ox}$), respectively, and 2 equiv of sodium in *n*-hexane.

As shown in Figure 2 for **5**, VTVH magnetic susceptibility measurements revealed that **3**, **5**, and **6** possess an $S = 1$

(17) (a) Becke, A. D. *J. Chem. Phys.* **1993**, *98*, 5648. (b) Becke, A. D. *J. Chem. Phys.* **1986**, *84*, 4524. (c) Lee, C. T.; Yang, W. T.; Parr, R. G. *Phys. Rev. B* **1988**, *37*, 785.
(18) Schäfer, A.; Horn, H.; Ahlrichs, R. *J. Chem. Phys.* **1992**, *97*, 2571.
(19) Schäfer, A.; Huber, C.; Ahlrichs, R. *J. Chem. Phys.* **1994**, *100*, 5829.
(20) Neese, F. *J. Phys. Chem. Solids* **2004**, *65*, 781.
(21) *Molekel, Advanced Interactive 3D-Graphics for Molecular Sciences*; available under http://www.cscs.ch/molekel/.
(22) Neese, F. *Inorg. Chim. Acta* **2002**, *337*, 181.
(23) Sinnecker, S.; Slep, L. D.; Bill, E.; Neese, F. *Inorg. Chem.* **2005**, *44*, 2245.
(24) Noodleman, L.; Norman, J. G. *J. Chem. Phys.* **1979**, *70*, 4903.
(25) Noodleman, L.; Peng, C. Y.; Case, D. A.; Mouesca, J. M. *Coord. Chem. Rev.* **1995**, *144*, 199.
(26) (a) Noodleman, L.; Case, D. A.; Aizman, A. *J. Am. Chem. Soc.* **1988**, *110*, 1001. (b) Noodleman, L.; Davidson, E. R. *Chem. Phys.* **1986**, *109*, 131. (c) Noodleman, L.; Norman, J. G.; Osborne, J. H.; Aizman, A.; Case, D. A. *J. Am. Chem. Soc.* **1985**, *107*, 3418. (d) Noodleman, L. *J. Chem. Phys.* **1981**, *74*, 5737.
(27) (a) Bachler, V.; Olbrich, G.; Neese, F.; Wieghardt, K. *Inorg. Chem.* **2002**, *41*, 4179. (b) Ghosh, P.; Bill, E.; Weyhermüller, T.; Neese, F.; Wieghardt, K. *J. Am. Chem. Soc.* **2003**, *125*, 1293.
(28) Blanchard, S.; Neese, F.; Bothe, E.; Bill, E.; Weyhermüller, T.; Wieghardt, K. *Inorg. Chem.* **2005**, *44*, 3636.
(29) (a) Herebian, D.; Bothe, E.; Neese, F.; Weyhermüller, T.; Wieghardt, K. *J. Am. Chem. Soc.* **2003**, *125*, 9116. (b) Herebian, D.; Wieghardt, K.; Neese, F. *J. Am. Chem. Soc.* **2003**, *125*, 10997.
(30) Slep, L. D.; Mijovilovich, A.; Meyer-Klaucke, W.; Weyhermüller, T.; Bill, E.; Bothe, E.; Neese, F.; Wieghardt, K. *J. Am. Chem. Soc.* **2003**, *125*, 15554.
(31) Chlopek, K.; Bothe, E.; Neese, F.; Weyhermüller, T.; Wieghardt, K. *Inorg. Chem.* **2006**, *45*, 6298.
(32) Patra. A. K.; Bill, E.; Bothe, E.; Chlopek, K.; Neese, F.; Weyhermüller, T.; Stobie, K.; Ward, M. D.; McCleverty, J. A.; Wieghardt, K. *Inorg. Chem.* **2006**, *45*, 7877.
(33) (a) Remenyi, C.; Kaupp, M. *J. Am. Chem. Soc.* **2005**, *127*, 11399. (b) Bencini, A.; Carbonera, C.; Dei, A.; Vaz, M. G. F. *Dalton Trans.* **2003**, 1701.
(34) Baker, R. J.; Farley, R. D.; Jones, C.; Mills, D. P.; Kloth, M.; Murphy, D. M. *Chem.−Eur. J.* **2005**, *11*, 2972.

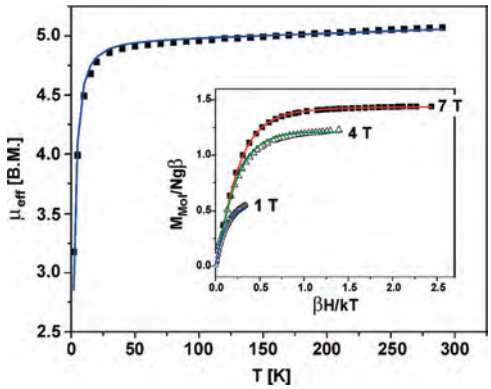

Figure 1. Temperature dependent magnetic moments, μ_{eff}/μ_B, and a variable temperature, variable field magnetization plot (inset) of $[Fe^{II}(^2L^{Ox})Cl_2]$ (**4**). (Simulation parameters are given in Table 2).

Table 2. Spin Hamiltonian Parameters from Variable Temperature, Variable Field (VTVH) Magnetic Susceptibility Measurements (1 T)

	S_t[a]	g	$\|D_t\|$, cm^{-1}[b]	$\|D_{Fe}\|$, cm^{-1}[c]
1	2	2.0	n.m.[d]	
2	2	2.01	7.7	7.7
3	1	2.06(fixed)	18.5	8.1
4	2	2.02	7.2	7.2
5	1	2.05(fixed)	16.1	7.7
6	1	2.30	16.2	8.1

[a] Ground state; [b] Zero-field splitting of S_t state; [c] Zero-field splitting parameter of intrinsic S_{Fe} state obtained by using spin projection techniques. [d] n.m. = not measured.

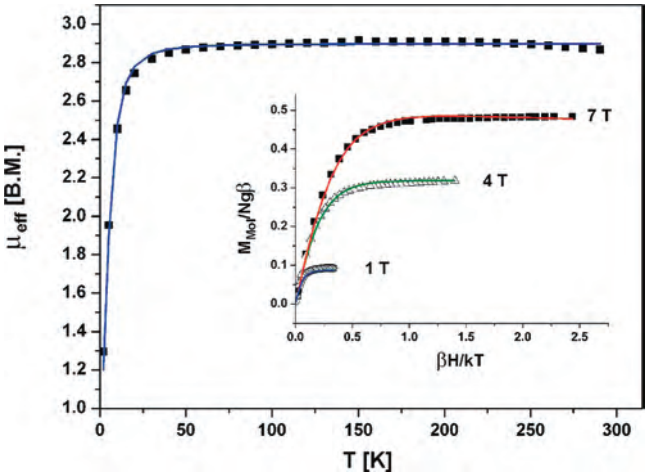

Figure 2. Temperature dependent magnetic moments, μ_{eff}/μ_B, and a VTVH magnetization plot (inset) of $[Fe^{II}(^2L^{\bullet})_2]$ (**5**). (Simulation parameters are given in Table 2). Similar plots of **3** and **6** are given in the Supporting Information.

ground state; the spin Hamiltonian parameters are summarized in Table 2. As we will show below, these neutral tetrahedral complexes possess a central high spin ferrous ion ($S_{Fe} = 2$) and two N,N′-coordinated ligand π radical anions ($S_{rad} = {}^1/_2$); the spins couple intramolecularly antiferromagnetically yielding the observed triplet ground state.

It is interesting that the zero-field splitting parameter $|D|$ values for the $S = 2$ complexes **2** and **4** are at ~7 cm^{-1} whereas the corresponding values $|D|_t$ for the $S = 1$ species **3**, **5**, and **6** are larger at ~17 cm^{-1}. The latter values may be converted to the intrinsic zero-field splitting parameter of the central iron ion ($S_{Fe} = 2$) $|D|_{Fe} \sim 7$ cm^{-1} by using spin

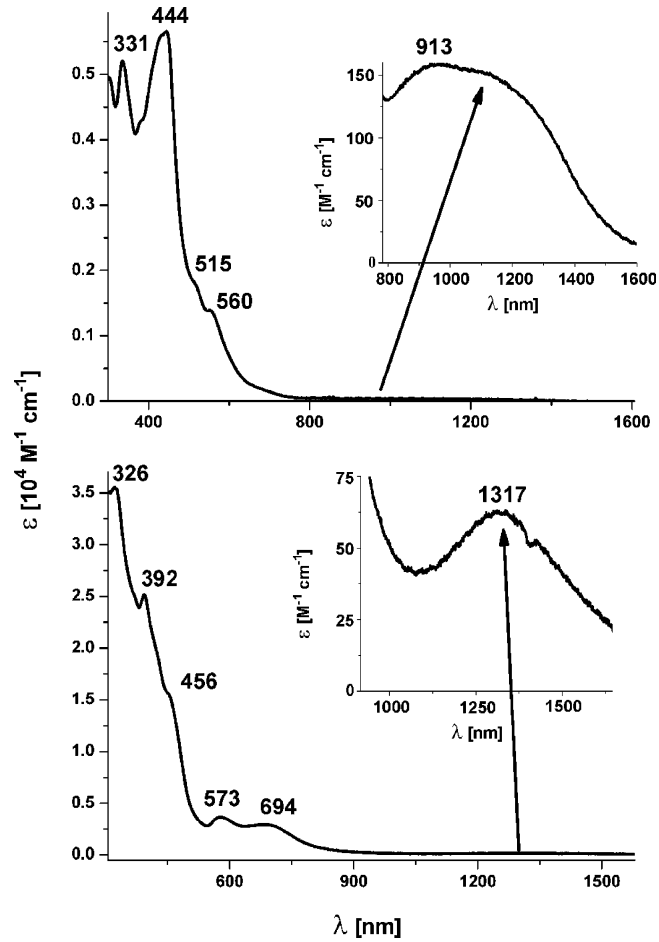

Figure 3. Electronic spectra of **3** (top) and **5** (bottom) in tetrahydrofuran.

Table 3. Electronic Spectra of Complexes in Tetrahydrofuran Solution at 20 °C

complex	λ, nm (ε, 10^4 M^{-1} cm^{-1})
1 ($S = 2$)	367(0.55), 495(0.8), 940(0.02)
2 ($S = 2$)	363(0.16), 551(0.03), 610(0.03)
3 ($S = 1$)	331(0.5), 441(0.6), 515(0.2), 560(0.15), 951(0.016), 1100sh (0.012)
4 ($S = 2$)	323(0.22), 359(0.20), 584(0.03), 648(0.04)
5 ($S = 1$)	326(3.55), 392(2.53), 456(1.55), 573(0.39), 694(0.3), 1317(0.006)
6 ($S = 1$)	392(0.8), 482sh(0.3), 550(0.2), 715(0.04), 990s(0.02), 1130sh(0.02)

projection techniques. They agree nicely with values for **2** and **4**. Thus, complexes **2**−**6** all contain a high spin ferrous ion in a tetrahedral ligand field.

Electronic spectra of complexes in tetrahydrofuran solution have been recorded at 20 °C; the results are summarized in Table 3. Figure 3 displays the spectrum of **3** (and **5**) which exhibits a weak ligand-to-ligand charge transfer band (LLCT) at ~1100 nm ($\varepsilon = 120$ M^{-1} cm^{-1}). This band is also present in the corresponding tetrahedral $[Ni(L^{\bullet})_2]$ complexes.[12a,35,36] Complex **5** displays this transition at 1317 nm ($\varepsilon = 60$ M^{-1} cm^{-1}). This LLCT band is spin-forbidden in tetrahedral $[Fe^{II}(L^{\bullet})_2]$ complexes and is therefore weak.[35] Similarly, in complex **6** this LLCT band has been identified at 1130 nm.

This transition is absent in the spectra of **1**, **2**, and **4** all of which contain closed shell ligands and a high spin ferrous

ion ($S_{Fe} = 2$). The LLCT band is therefore considered to be a spectroscopic marker for the presence of two ligand π radicals in $[Fe^{II}(L^{\bullet})_2]^0$ species.

We have also prepared Chirik's complexes **7**, **8**, and **9** (Scheme 3) according to the reported procedures[4] to investigate more completely the electronic structure of these complexes and recorded their Mössbauer spectra (see below). These complexes contain the ArN=C(CH_3)−C(CH_3)=NAr (Ar = 2,6-diisopropylphenyl) ligand ($^5L^{Ox}$). $[Fe^{II}(^5L^{Ox})Cl_2]$ (**7**) is the exact analog of complexes **2** and **4** which all contain a high spin ferrous ion and a neutral α-diimine ligand, as well as two chloride ligands in a tetrahedral geometry. In accord with this, the magnetic susceptibility data of **7** indicate also an $S = 2$ ground state.

The complex **8** containing two α-diimine type radical monoanions (our interpretation as we will show below) and a high spin ferrous ion ($S_{Fe} = 2$) possesses a triplet ground state ($S_t = 1$). Note that the authors in ref 4a prefer to describe its electronic structure as a tetrahedral iron(0) d^8 complex containing two closed-shell α-diimine ligands or as an intermediate-spin iron(III) d^5 complex where one α-diimine acts as a closed-shell, strong field, dianionic ligand and the second as a monoanionic π radical. The reported crystal structure determination of **8** is inconclusive and appears to be flawed because the two C−N bonds within each bidentate ligand are found to be inequivalent(!) at 1.35(1) and 1.43(1) Å (1.28(1) and 1.35(1) Å in the other ligand).[37]

Finally, reduction of **7** with $LiCH_2CHMe_2$ yields the dimer **9** which has been characterized by X-ray crystallography.[4b] Two tetrahedrons are bridged by two chloride ligands (edge-sharing).

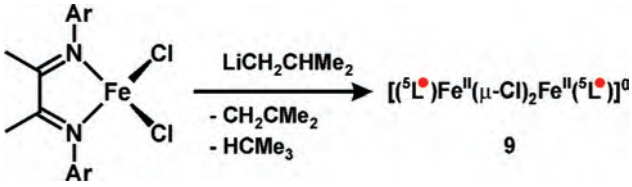

We have measured its temperature-dependent molar magnetic susceptibility in a 1.0 T magnetic field. The temperature-dependent magnetic moments of **9** in the range 2−295 K are shown in Figure 4; they display a continual increase from 0.9 μ_B at 2 K to 5.4 μ_B at 295 K, revealing the presence of a large number of well spread spin sublevels in the corresponding energy range.

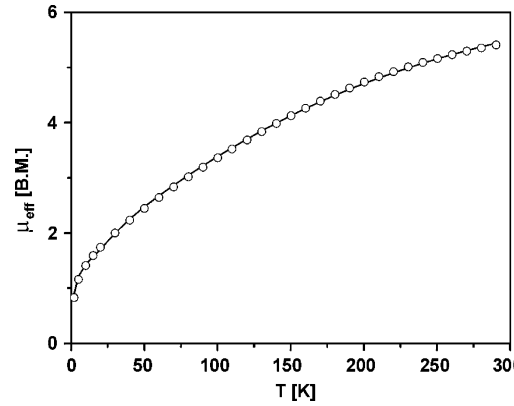

Figure 4. Temperature-dependence of magnetic moments of **9** (experimental data). The solid line represents a best fit of the data (see text).

Table 4. Experimental and Calculated Bond Distances (Å) of **1**

	exp.	calcd.
Fe1−N1	2.083(1)	2.126
Fe1−N2	1.972(1)	2.014
N1−C1	1.331(2)	1.326
N1−C9	1.370(2)	1.364
N2−C8	1.366(2)	1.365
N2−C10	1.474(2)	1.481
C1−C2	1.394(2)	1.409
C2−C3	1.372(2)	1.381
C3−C4	1.413(2)	1.421
C4−C5	1.415(2)	1.418
C4−C9	1.417(2)	1.433
C5−C6	1.365(2)	1.383
C6−C7	1.403(2)	1.410
C7−C8	1.401(2)	1.413
C8−C9	1.452(2)	1.463
θ, deg[a]	87	88.8

[a] Dihedral angle between two five-membered chelate rings.

It has not been possible to simulate the data satisfactorily by using a model where only two effective spins $S^* = {}^3/_2$ (arising from a very strong antiferromagnetic exchange coupling of a high spin ferrous ion coordinated to a ligand radical ($S_{Fe} = 2$ and $S_{rad} = {}^1/_2$)) are intramolecularly antiferromagnetically exchange coupled. On the other hand, if the ligand-to-metal interaction is not predominant, one can explicitly consider this by using a model which involves a spin tetramer $L^{\bullet}\cdots Fe^{II}\cdots Fe^{II}\cdots L^{\bullet}$ with two terminal ligand radicals $(^5L^{\bullet})^{1-}$ ($S_{rad} = {}^1/_2$) and two high spin ferrous ions ($S_{Fe} = 2$). By using the spin-Hamiltonian in eq 1 and including a 9% paramagnetic impurity ($S = {}^5/_2$) as indicated by the Mössbauer spectrum and a fixed zero-field splitting for the iron(II) sites ($|D| = 12 \pm 5$ cm^{-1}), the following exchange coupling constants were obtained from a best fit: $J = J_1 = J_3 = -53$ cm^{-1} for the iron-radical interaction and $J' = J_2 = -25$ cm^{-1} for the iron−iron coupling.

X-ray Crystal Structures. The structures of **1**, **2**, and **6** have been determined by single crystal X-ray crystallography at 100(2) K. Crystallographic data are summarized in Table 1 and selected bond distances are given in Tables 4 and 5. Figures 5, 6, and 7 show the structures of **1**, **2**, and **6**, respectively.

(35) Muresan, N.; Weyhermüller, T.; Wieghardt, K. *Dalton Trans.* **2007**, 4390.

(36) (a) tom Dieck, H.; Svoboda, M.; Greiser, Z. *Z. Naturforsch.* **1981**, *36b*, 823. (b) Svoboda, M.; tom Dieck, H.; Krüger, C.; Tsay, Y.-H. *Z. Naturforsch.* **1981**, *36b*, 814. (c) Bonrath, W.; Pörschke, K. R.; Mynott, R.; Krüger, C. *Z. Naturforsch.* **1990**, *45b*, 1647.

(37) No crystallographic details for **8** have been given in the text of ref 4a (which is compound **4** in this paper). Retrieval from the supporting information material and a closer inspection of the CIF-file, which has been deposited with the Cambridge Crystallographic Data Center, revealed that the compound has been refined in an incorrect space group. Although the correct space group *P*2/*n* (No.13) is given in the crystallographic table and the CIF-file, the compound was actually refined in the non-centrosymmetric space-group *Pn* (No.7) and these data were used to calculate bond distances. The missing crystallographic C_2 axis brings about the apparent inequivalence of the C−N bond distances in the chelate rings and the suspicious thermal displacement parameters.

Table 5. Calculated and Experimental Bond Distances (Å) of Five-Membered Chelate Rings and Dihedral Angles θ (deg) between Chelate Rings in FeL_2 Complexes (L = α-diimine)

	3 (calcd)	**5** (calcd)	$[Fe^{II}(^{5'}L^{\bullet})_2]$ (calcd)	*transoid*-**6** (exp.)	*transoid*-**6** (calcd)
Fe−N1	2.038	2.108	2.058	2.013(2)	2.051
Fe−N4	2.006	2.088	2.049	2.025(2)	2.049
Fe−N21	2.028	2.103	2.059	disordered	2.056
Fe−N24	2.014	2.090	2.049	disordered	2.051
N1−C2	1.348	1.345	1.347	1.343(2)	1.341
C2−C3	1.420	1.412	1.431	1.408(3)	1.419
C3−N4	1.336	1.338	1.347	1.341(2)	1.341
N21−C22	1.350	1.346	1.344	disordered	1.341
C22−C23	1.420	1.413	1.431	disordered	1.420
C23−N24	1.335	1.337	1.349	disordered	1.340
θ, deg [a]	88	56	79	73.0	76.4

[a] Dihedral angle between chelate rings.

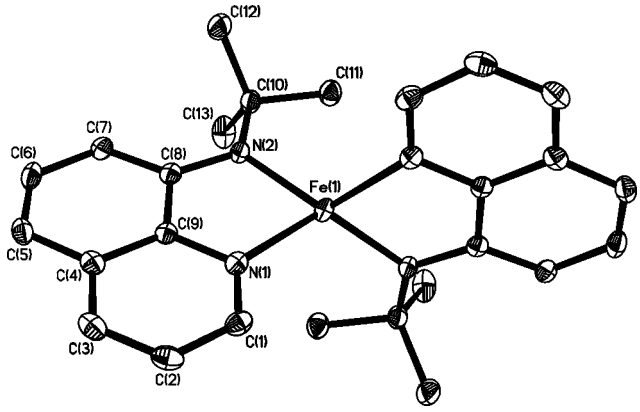

Figure 5. Structure of a neutral molecule in crystals of **1** (hydrogen atoms were omitted; thermal ellipsoids are drawn at the 50% level).

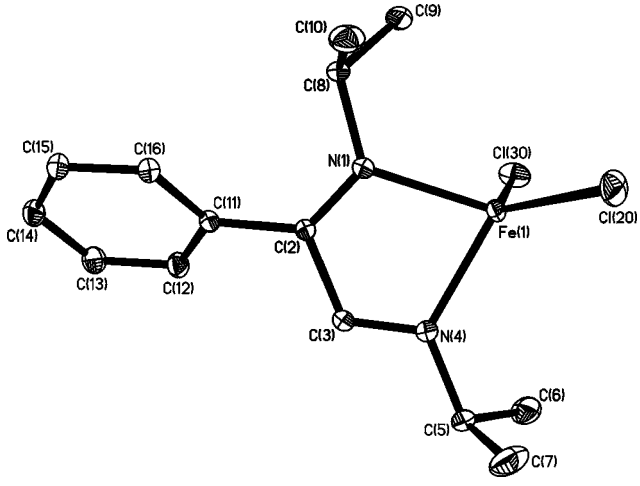

Figure 6. Structure of a neutral molecule in crystals of **2** (thermal ellipsoids are at the 50% level).

Neutral molecules $[Fe^{II}(^4L)_2]$ in crystals of **1** contain two N,N′-coordinated monoanionic *N-tert*-butylquinolinylamide and a high spin ferrous ion. The FeN_4 coordination polyhedron is a tetrahedron where the two $N_{amide}-Fe-N_{py}$ planes form a dihedral angle θ of 87° (it is 90° in a regular tetrahedron and 0° in a square planar arrangement). The average $Fe-N_{amide}$ and $Fe-N_{py}$ distance at 1.986 and 2.083 Å, respectively, are long and consistent with four-coordinated high spin Fe^{II}. The C−C and C−N bond lengths of the ligands are unexceptional and in the usual range observed for quinolines. This indicates that the closed-shell monoanions $(^4L)^{1-}$ in **1** are redox-innocent. Thus, complex **1** serves as a benchmark for a tetrahedral, high spin ferrous species ($S = 2$) with an FeN_4 polyhedron.

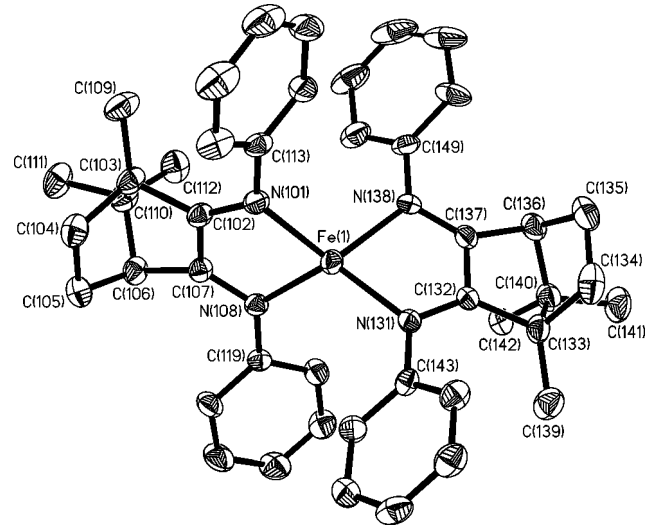

Figure 7. Structure of the *transoid* form of **6** (that of the *cisoid* form is not shown).

Neutral molecules $[Fe^{II}(^1L^{Ox})Cl_2]$ in crystals of **2** contain a four coordinate, high spin ferrous ion with a neutral N,N′-coordinated α-diimine ligand $(^1L^{Ox})^0$ and two chloride ligands. The FeN_2Cl_2 polyhedron is distorted tetrahedral; the two planes $FeCl_2$ and FeN_2 form a dihedral angle of 88.9°. The average Fe−N and Fe−Cl bond lengths are long at 2.112 and 2.239 Å, respectively; they indicate a high spin configuration at the central Fe^{II} ($S = 2$). Two very similar structures have recently been reported by Gibson et al.[38] It is now very gratifying that the average C−N bond length of the ligand $(^1L^{Ox})^0$ at 1.284 Å in **2** corresponds to a *C*═N double bond, whereas the distance C2−C3 at 1.501 Å is a typical single bond. The oxidation level of the α-diimine ligand is therefore that of neutral $(^1L^{Ox})^0$ as shown in Schemes 1 and 2. Thus, complex **2** serves as a benchmark for a closed shell, neutral α-diimine ligand coordinated to a high spin ferrous ion.

Complex **6** crystallizes in the chiral monoclinic space group $P2_1$ with two crystallographically independent neutral molecules $[Fe^{II}(^3L^{\bullet})_2]$ in the unit cell. Interestingly, these molecules display a static disorder comprising the *transoid*- and *cisoid*-isomer which exist only if the dihedral angle θ between the two five-membered chelate rings is $\neq 90°$.

In both independent molecules only one of the ligands is disordered. Because a number of restraints had to be introduced to refine a split atom model, metrical parameters of the disordered parts are less reliable. In the following we will therefore discuss the structural parameters of the nondisordered part of the *transoid*-isomer only. The averaged dihedral angle θ of the two independent molecules in **6** is 73.0°. The FeN_4 polyhedron is distorted tetrahedral, and the average Fe−N bond length at 2.02 Å is long and indicates

(38) Allan, L. E. N.; Shaver, M. P.; White, A. J. P.; Gibson, V. C. *Inorg. Chem.* **2007**, *46*, 8963.

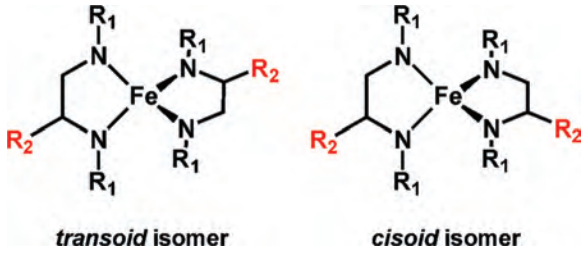

the presence of a high spin ferrous ion ($S_{Fe} = 2$). The two ligands are identical within the 3σ standard deviation limit of the C−C and C−N bond distances. The oxidation level of the two α-diimines is clearly that of a π radical monoanion $(^3L^{\bullet})^{1-}$ as shown in Scheme 2 because the average C−N distance at 1.342 Å is intermediate between an α-diimine $(^3L^{Ox})^0$ at ∼1.29 Å and an enediamide $(^3L^{Red})^{2-}$ at 1.38 Å. Similarly, the av C−C distance at 1.408 Å is intermediate between that in $(^3L^{Ox})^0$ and $(^3L^{Red})^{2-}$. We note that the quality of the present structure determination of **6** is significantly better than that of complex **8** in ref 4. Here the two C−N distances in either of the two ligands are identical.

An excellent crystal structure determination of complex **9**[4] has been reported. This complex contains two edge-sharing $LFeCl_2$ tetrahedral units. Interestingly, the reported C−C and C−N distances of the α-diimine ligand shown in Figure 8 are in excellent agreement with the data for a π radical anion $(^5L^{\bullet})^{1-}$ (Scheme 2). This implies that the central metal ion possesses a +II oxidation level (high spin ferrous as was deduced from the magnetic data).

Mössbauer Spectroscopy. Zero-field Mössbauer spectra of polycrystalline samples were recorded at 80 K; the results are summarized in Table 6 and 7 The spectra of **1**−**5** consist of a doublet from a major component (>80%) and a minor doublet from some unknown impurities (<20%). It is now important that the spectra of the tetrahedral high spin species **1**, **2**, and **4** with an $S = 2$ ground-state exhibit very similar large isomer shift values δ in the range 0.77−1.02 mm s^{-1} and large quadrupole splitting parameters in the range 2.14−3.13 mm s^{-1}. These values are characteristic for high spin ferrous species ($S_{Fe} = 2$) in a tetrahedral ligand field.

The tetrahedral complexes **3**, **5**, and **6** possess an $S = 1$ ground state. The isomer shift values of these species are observed in the narrow range 0.50−0.70 mm s^{-1}; the quadrupole splitting parameters are very large in the range 2.82−4.28 mm s^{-1}. This set of data points again to the presence of high

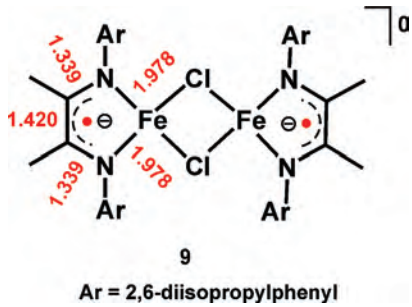

Figure 8. Crystallographic data for complex **9** from ref 4. Bond distances are given in Å.

Table 6. Mössbauer Parameters of Complexes at 80 K[a]

complex	S_t[b]	δ, mm s^{-1}[c]	$\lvert\Delta E_Q\rvert$, mm s^{-1}[d]	%[e]
1	2	0.77(0.70)	2.14(2.15)	94.2
		0.48	0.6	5.8
2	2	0.89	2.78	100
3	1	0.50(0.51)	4.28(4.45)	91.7
		0.43	0.83	8.3
4	2	1.02	3.13	83
		0.97	2.52	17
5	1	0.59(0.68)	2.82(2.95)	91.2
		0.43	0.83	8.8
6	1	0.65(0.51)	4.19(4.43)	58 *transoid*
		0.65	3.62	40 *cisoid*

[a] Values given in parentheses are calculated ones (B3LYP). [b] Ground state. [c] Isomer shift vs α-Fe (298 K). [d] Quadrupole splitting. [e] Amount of major and minor component (subspectra **a** and **b**).

Table 7. Zero-field Mössbauer Data of Complexes **7**, **8**, **9** at 80 K[a]

complex	S_t[b]	S_{Fe}[c]	δ, mm s^{-1}[d]	$\lvert\Delta E_Q\rvert$, mm s^{-1}[e]
7	2	2	0.84	2.57
8	1	2	0.77(0.73)	1.81(2.08)
9	0[f]	2	0.88	2.68

[a] Values in parenthesis were calculated. [b] Ground-state of molecule. [c] Intrinsic spin state of central iron ion. [d] Isomer shift vs α-Fe (298 K). [e] Quadrupole splitting. [f] Antiferromagnetic coupling of two high spin ferrous ions (see text).

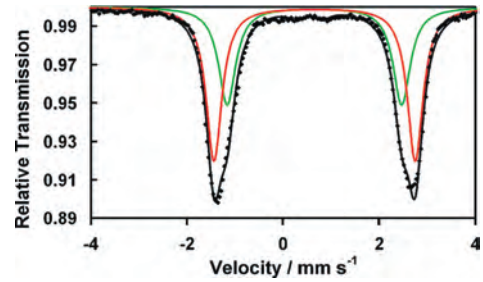

Figure 9. Zero-field Mössbauer spectrum of **6** at 80 K: Subspectrum **a** (40%) may correspond to the *cisoid* form of the neutral molecule in **6** whereas that of **b** (58%) may be due to the corresponding *transoid* isomer.

spin ferrous ions ($S_{Fe} = 2$). (We note that to the best of our knowledge there are no authenticated Mössbauer parameters for a genuine Fe(0) (d^8) species with an $S = 1$ spin state.)

Interestingly, as shown in Figure 9 the zero-field Mössbauer spectrum at 80 K of solid **6** consists of two very similar quadrupole doublets, namely subspectrum **a** (∼40%) with $\delta = 0.65$ mm s^{-1} and $\Delta E_Q = 3.62$ mm s^{-1} and subspectrum **b** with $\delta = 0.65$ mm s^{-1} and $\Delta E_Q = 4.19$ mm s^{-1} (∼58%). A third subspectrum **c** (∼2.5%) with $\delta = 0.55$ mm s^{-1} and $\Delta E_Q = 0.53$ mm s^{-1} is probably due to a high spin ferric species produced via oxidatiave degradation of **6** with air. Subspectrum **a** corresponds to the *cisoid* form of **6** whereas that of **b** is probably the spectrum of the *transoid* form. This would be in agreement with the X-ray crystallographic results (vide supra).

Figure 10 displays magnetically perturbed Mössbauer spectra of **3**. For the simulations the following parameters from magnetic susceptibility measurements were used (Table 2): $g_x = g_y = g_z = 2.06$; $|D| = 18.5$ cm^{-1}, $S_t = 1$; $E/D = 0$. The results give $\delta = 0.50$ mm s^{-1}, $\Delta E_Q = -4.28$ mm s^{-1} (at 4.2 K); an asymmetry parameter $\eta = 0.2$; $A/g_N\beta_N(S_t)$, $T = (-11.0, -16.0, -32.0)$. By using spin projection techniques it is possible to convert the magnetic hyperfine tensor values $A/g_N\beta_N$ ($S_t = 1$) to the intrinsic values which are

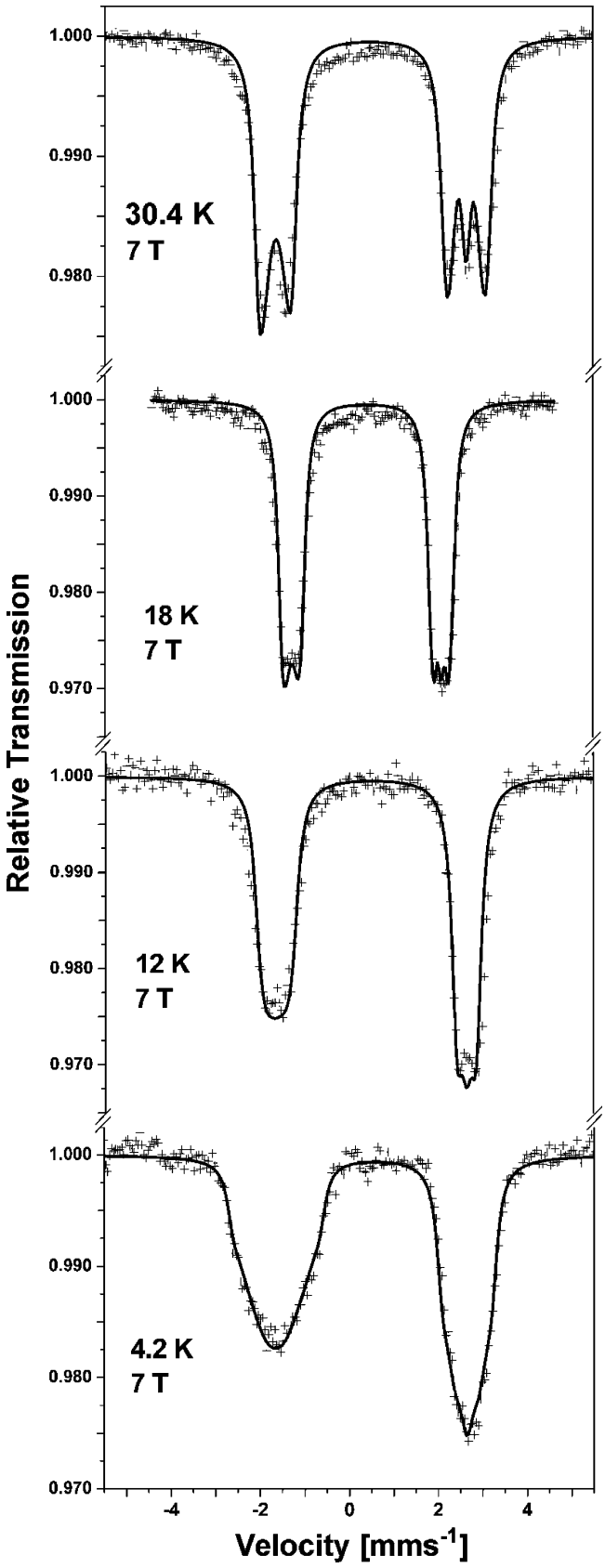

Figure 10. Mössbauer spectra of **3** with B = 7T applied perpendicular to the γ-ray.

characteristic for the local spin state of the ferrous ion (S_{Fe} = 2): $A/g_N\beta_N$ (S_{Fe} = 2) = (−7.3, −10.7, −21.3) T. These values are quite typical for a high spin ferrous ion.

Zero-field Mössbauer data for complexes **7**, **8**, and **9** are summarized in Table 7. The high isomer shift values of all three species clearly point to the presence of high spin ferrous ions (S_{Fe} = 2) in all three cases. This implies that **7** contains a neutral α-diimine ligand [$Fe^{II}(^5L^{Ox})Cl_2$] whereas **8** contains two π radical monoanions as in [$Fe^{II}(^5L^{\bullet})_2$]. Most interestingly, the dimeric complex **9** must also contain two high spin ferrous ions and two ligand π radical anions.

DFT Calculations. a. Optimized Geometries for 1, 3, 5, and [$Fe^{II}(^{5'}L^{\bullet})_2$]. The tetrahedral complex **1** possesses an S = 2 ground state. We optimized its ground-state geometry assuming the presence of a high spin, open shell S = 2 state by using the spin-unrestricted Kohn−Sham functional B3LYP. The experimental and calculated geometric structures are in excellent agreement (Table 4); the C−C and C−N bond distances agree within ±0.01 Å whereas the calculated Fe−N bond distances are overestimated by ∼0.04 Å which is a typical result for the B3LYP functional. It is also remarkable that the calculated dihedral angle θ between the two five-membered Fe−N−C−C−N chelate rings at 88.8° is in excellent agreement with the experimental value of 87°.

Tetrahedral complexes **3**, **5**, **6**, and [$Fe^{II}(^{5'}L^{\bullet})_2$], the latter of which is the truncated model of complex [$Fe^{II}(^5L^{\bullet})_2$] (Scheme 3)[4] where the i-propyl groups have been replaced by hydrogen atoms, possess a triplet ground state. Therefore, we have calculated the following models: (a) a standard spin-unrestricted S = 1 model; (b) a broken symmetry BS(4,2) M_S = 1 model for a high spin ferrous ion (S_{Fe} = 2) and two antiferromagnetically coupled ligand π radicals (S_{rad} = $^1/_2$), and (c) a BS(3,1) M_S = 1 model implying the presence of an intermediate spin ferric ion (S_{Fe} = $^3/_2$), one ligand π radical, $(L^{\bullet})^{1-}$, and one closed shell enediamide ligand $(L^{Red})^{2-}$. Interestingly, all three models for each complex converged to the same isoenergetic and isostructural solution of the BS(4,2) minimum. The adiabatically excited BS(6,0) model was found to be ∼11 kcal mol higher in energy than the corresponding BS(4,2) solution.

Table 5 summarizes the calculated metrical details of the two five-membered chelate rings Fe−N−C−C−N in **3**, **5**, *transoid*-**6**, and [$Fe^{II}(^{5'}L^{\bullet})_2$]. It is remarkable that irrespective of the N-substituents of the respective α-diimine or of the carbon backbone, the C−N and C−C bond lengths of the five-membered chelate rings are within a very small range identical with those reported for the monoanionic π radical form in Scheme 2. Experimentally this backbone has the same bond lengths in **6**. Therefore, we conclude that the structural data (calculated or experimental) are in excellent agreement with the presence of two monoanionic ligand π radicals $(^xL^{\bullet})^{1-}$ in these complexes.

We note that the dihedral angle θ between the two five-membered chelate rings is strongly influenced by the steric bulk of the N-substituents and varies from 88° in **3** to 56° in **5**. The smaller this substituent is, the more tetrahedral is the FeN_4 polyhedron ($\theta \rightarrow 90°$).

b. Electronic Structures of 1, 3, 5, transoid-6, and [$Fe^{II}(^{5'}L^{\bullet})_2$]. For pseudotetrahedral **1**, the molecular orbital (MO) bonding scheme (Supporting Information) shows the pres-

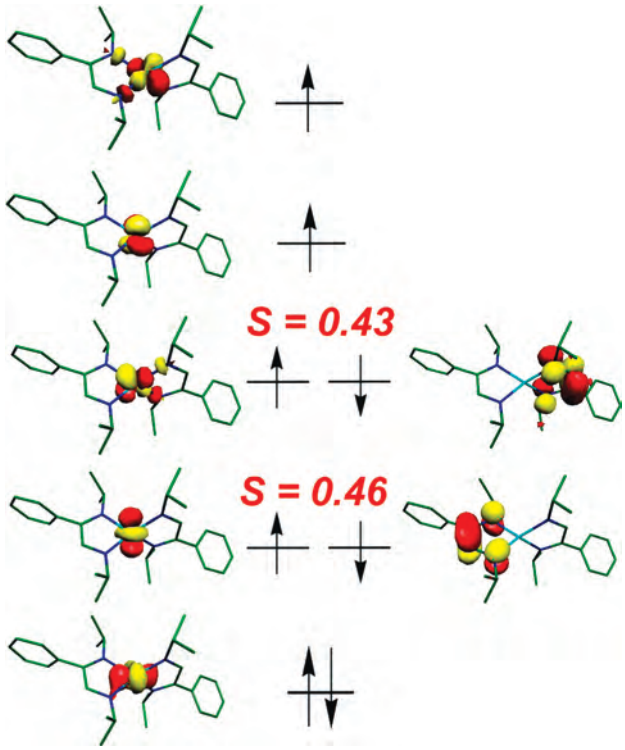

Figure 11. Qualitative MO diagram of the magnetic orbitals derived from BS(4,2) calculation of **3**. The spatial overlap (*S*) of corresponding alpha and beta orbitals is given.

ence of a central (higher spin) ferrous ion: the five highest energy orbitals are of predominantly metal-d character, one of which is doubly occupied, and four are singly occupied as one expects for an $S = 2$ Fe(II) ion in a tetrahedral ligand field. The Mulliken spin population analysis corroborates this notion: ~3.8 unpaired electrons are located at the ferrous ion and no spin density resides on the ligands. Thus, **1** is a classical Werner-type coordination compound.

A qualitative MO bonding scheme derived from the spin-unrestricted BS(4,2) calculation for **3** is shown in Figure 11. Five orbitals of predominantly metal-d character are again identified. One of them is found in the spin-up *and* spin-down manifolds; it is doubly occupied. The other four Fe-based orbitals occur only in the spin-up manifold. These four orbitals are thus singly occupied with parallel spins (Fe(II); $S_{Fe} = 2$). In addition, two ligand centered orbitals are identified in the spin-down manifold which are not populated in the spin-up manifold. This situation leads to the observed overall $M_S = 1$ state. These orbitals correspond to two symmetry-adapted combinations of the singly occupied molecular orbital (SOMO) of the two ligand π radicals. Complex **3** features a high spin Fe(II) ion which is antiferromagnetically coupled to two ligand-centered π radical monoanions.

The spin density plot (Mulliken analysis) in Figure 12 nicely shows the antiparallel spin alignment between the high spin Fe(II) (positive spin density in red) and the π radical ligands (negative spin density in yellow). An approximate breakdown of the spin density into atomic contributions via a spin population analysis supports the presence of four unpaired electrons at the iron ion with a positive spin and

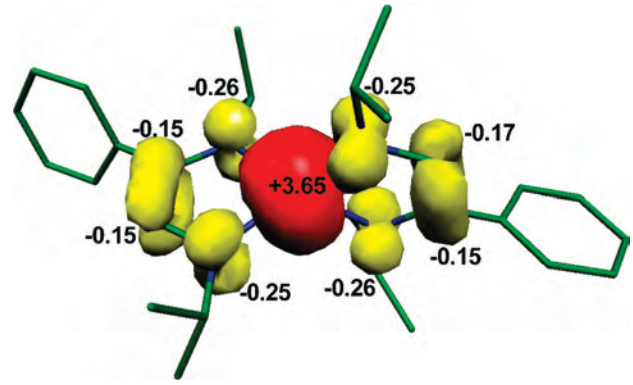

Figure 12. Spin-density plot shown with values as derived from the BS(4,2) calculation of **3** (based on a Mulliken spin population analysis).

two unpaired electrons with a negative spin localized on the two ligand π radicals.

The corresponding orbital transformation is used to visualize the overlapping magnetic pairs of the system.[20] The spin-orbitals obtained from single-point unrestricted calculations were transformed in such a way that for each spin-up orbital there exists at most one spin-down partner that has nonzero spatial overlap. Values of S close to 1 indicate a standard doubly occupied MO with little spin-polarization, whereas $S \ll 1$ is the signature of nonorthogonal magnetic orbital pairs. For **3** two such magnetically interacting pairs which interact via a π pathway have been identified. Each of these pairs consists of one metal orbital and the corresponding ligand radical orbital.

The computational electronic structure results for $[Fe^{II}(^{5'}L^{\bullet})_2]$ and *transoid*-**6** (Supporting Information) give exactly the same model as shown above for **3**. Two ligand π radicals are intramolecularly antiferromagnetically coupled to a high spin ferrous ion yielding the observed triplet ground state.

To calibrate the above calculated electronic structures, we have calculated the Mössbauer spectra[22,23] of selected complexes, namely those of **1**, **3**, **5**, *transoid*-**6**, and of complex **8**. The results are summarized in Table 6 and 7. It is quite remarkable how well the experimental and calculated values agree. For *transoid*-**6** the calculated and experimental geometric structure and Mössbauer parameters are in good agreement giving confidence in the correct evaluation of the electronic structures for **3**, for **5** where X-ray structures are not available, and for **8** where the crystal structure is flawed.[37] Thus, all present bis(α-diimine)iron complexes (**3**, **5**, **6**, and **8**) with a triplet ground-state must be described as high-spin ferrous species N,N′-coordinated to two π radical monoanions $(L^{\bullet})^{1-}$ where strong intramolecular antiferromagnetic spin-coupling yields the observed $S = 1$ ground state.

Conclusion

From a combination of structural and spectroscopic investigations in conjunction with broken-symmetry DFT calculations it has been possible to unequivocally establish the following electronic structures for a variety of iron

complexes containing α-diimine type ligands in two different oxidation levels, namely neutral ligand $(^{x}L^{Ox})^{0}$ and monoanionic π radicals $(^{x}L^{\bullet})^{1-}$.

(1) The tetrahedral, neutral complex **1** ($S = 2$) is a typical Werner-type complex with a central high-spin ferrous ion and two closed-shell, monoanionic *N-tert*-butylquinolinylamide ligand. Four unpaired electrons are located in metal-d orbitals, and no spin density has been detected on the ligands.

(2) The tetrahedral neutral complexes ($S = 2$) **2**, **4**, and **7** also contain a central ferrous ion coordinated to two chloride ions and one neutral, closed-shell α-diimine ligand (the average C−N bond is found at 1.29 Å).

(3) The most salient feature of the present study is the discovery that the neutral bis(α-diimine)iron complexes **3**, **5**, **6**, and **8** with a triplet ground-state all consist of a high-spin ferrous ion ($S_{Fe} = 2$) N,N′-coordinated to two α-diiminate(1−) π radicals ($S_{rad} = {}^{1}/_{2}$). The observed triplet ground-state is attained via intramolecular antiferromagnetic spin−spin coupling between the ligand π radicals and the ferrous ion. BS(4,2) DFT calculations clearly show (from a Mulliken spin population analysis) α-spin density on both ligands (∼2 unpaired electrons) and β-spin density at the central metal ion (4 unpaired electrons). There is no spectroscopic or DFT calculational evidence for the description as low-valent Fe(0) with two diamagnetic α-diimine ligands.

(4) As a consequence of this study, the electronic structure descriptions of complexes **7**, **8**, and **9** need to be revised. Complex **7** is a previously described[4] high-spin ferrous complex ($S = 2$) with an N,N′-coordinated neutral α-diimine ligand and two coordinated chloride anions. Complex **8** is also a high-spin ferrous species but N,N′-coordinated to two α-diiminate π radical anions. Finally, dimeric **9** contains two high-spin ferrous ions and two π radical monoanionic ligands $(^{5}L^{\bullet})^{1-}$ yielding, via intramolecular antiferromagnetic exchange coupling, the observed $S = 0$ ground state.

Acknowledgment. N.M. and M.G. are grateful to the Max-Planck Society for a postdoctoral stipend and C.C.L. thanks the A. v. Humboldt Foundation for a fellowship. We gratefully acknowledge financial support from the Fonds of the Chemical Industry. M.A. thanks the Caltech SURF program for funding. We also would like to thank Dr. K. Chlopek for preliminary DFT calculations of **8**.

Supporting Information Available: X-ray crystallographic files in CIF format for **1**, **2**, and **6** and tables of geometrical and electronic structural details of BS DFT calculated structures (PDF). Figures S1 and S2 display temperature dependent magnetic susceptibility data of **2** and **6**; Figures S3 and S4 show disorder models of **6**. This material is available free of charge via the Internet at http://pubs.acs.org.

IC7022693